Distribution of M-Wave and H-Reflex in Hand Muscles Evoked via Transcutaneous Nerve Stimulation: A Preliminary Report

Luis Vargas, John Baratta, and Xiaogang Hu

Abstract—**Neuromuscular electrical stimulation (NMES) targeting the muscle belly is commonly used to restore muscle strength in individuals with neurological disorders. However, early onset of muscle fatigue is a major limiting factor. Transcutaneous nerve stimulation (TNS) can delay muscle fatigue compared with traditional NMES techniques. However, the recruitment of Ia afferent fibers has not be specifically targeted to maximize muscle activation through the reflex pathway, which can lead to more orderly recruitment of motor units, further delaying fatigue. This preliminary study assessed the distribution of M-wave and H-reflex of intrinsic and extrinsic finger muscles. TNS was delivered using an electrode array placed along the medial side of the upper arm. Selective electrode pairs targeted the median and ulnar nerves innervating the finger flexors. High-density electromyography (HD EMG) was utilized to quantify the spatial distribution of the elicited activation of finger intrinsic and extrinsic muscles along the hand and forearm. The spatial patterns were characterized through isolation of the M-wave and H-reflex across various stimulation levels and EMG channels. Our preliminary results showed that, by altering the stimulation amplitude, distinct M-wave and H-reflex responses were evoked across EMG channels. In addition, distinct stimulation locations appeared to result in varied levels of reflex recruitment. Our findings indicate that it is possible to adjust stimulation parameters to maximize reflex activation, which can potentially facilitate physiological recruitment order of motoneurons.**

I. Introduction

A common symptom among many neurological disorders is hand muscle weakness or paralysis of the hand [1]. Impaired hand function can limit an individual's quality of life and their independence. Stroke, for instance, is the leading cause of disability in adults worldwide with approximately 795,000 cases occurring each year in the United States [2]. Following a stroke, around 66% of stroke survivors will experience muscle weakness in their upper limbs, notably in their hands [3], [4].

Rehabilitative or assistive tools, such as neuromuscular electrical stimulation (NMES), are often employed to combat muscle weakness [5]. Using large stimulation electrodes near the innervation zone of the muscle belly, NMES typically activates the muscles by stimulating distal branches of the motor axons near the innervation points. Although promising, NMES is limited as it causes the stimulated muscle to rapidly fatigue due to the non-physiological activation of the muscle

fibers [6]. Namely, the motor units are activated either in a random order or in a reverse order relative to the size principle as in voluntary activation [7], and only superficial muscle regions close to the stimulation electrodes are activated. This can limit the utility of NMES across clinical applications.

Instead of targeting innervation zone as in NMES, transcutaneous nerve stimulation (TNS) directly activates peripheral nerve bundles, which can elicit muscle contraction by activating the efferent fibers that directly innervate the muscles and the afferent fibers that make synaptic connections with the motoneurons of the targeted muscles [8]. TNS can lead to the recruitment of a greater spatial distribution of fatigable and non-fatigable fibers [9] in both deep and superficial muscles, which can distribute the burden required to produce a given motion [10]. Recent work has shown that TNS applied to the proximal segments of the median and ulnar nerve can elicit various hand gestures in neurologically intact [11] and stroke [12] individuals. One major benefit of TNS is the possibility of activating Ia afferent fibers to elicit H-reflex activities [13], which leads to orderly recruitment following the size principle, thereby delaying fatigue onset. Previous studies have assessed the maximum reflex amplitude, H-reflex reliability, and H-reflex threshold in paretic and non-paretic limbs using a single channel of EMG [14], [15]. However, we have limited knowledge regarding the muscle activation pattern elicited through efferent and afferent pathways of the hand muscles, when stimulation intensity and location varies.

Accordingly, the purpose of this study was to evaluate the distribution of M-wave and H-reflex in intrinsic and extrinsic finger muscles with various stimulation location and intensity. A 2×8 stimulation grid was placed along the medial side of the upper arm to target the median and ulnar nerve bundles. Distinct electrode pairs can produce unique electric field that
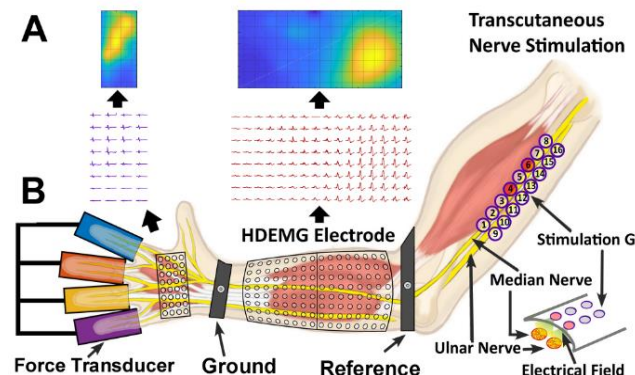

Figure 1. Diagram illustrating the experimental setup detailing the placement of the HD-EMG along the hand and forearm as well as the 2×8 stimulation electrode grid (B). Representative heat maps and evoked muscle activities from a single stimulation pulse (A) depict the EMG activation elicited through transcutaneous nerve stimulation.

can activate different set of efferent and afferent fibers. By varying the stimulation intensity, we constructed the M-wave and H-reflex recruitment curves. To capture muscle activation patterns, we used two high-density electromyogram (HD EMG) electrode grids over the intrinsic and extrinsic finger flexors, which can provide detailed information of the evoked responses, including the spatial distribution across the muscles. Using the stimulation and recording approaches, this preliminary work can characterize direct motor nerve and reflex activations using TNS. The outcomes can be used to guide stimulation protocols that can maximize reflex activation, in order to enable physiological recruitment order of motoneurons and reduce the degree of muscle fatigue. This can permit long-term use of TNS, facilitate recovery of muscle strength, and eventually promote improved quality of life for individuals with neuromuscular deficiencies.

II. METHODS

A. Subjects

Two participants with no known neurological disorders were recruited. Both participants gave informed consent via protocols approved by the Institutional Review Board of the University of North Carolina at Chapel Hill.

B. Experimental Setup

Participants were seated in a height adjustable chair with their right arm comfortably placed on a table in front of them. To improve conductivity of the stimulation grid, the skin over the medial portion of the upper arm was cleaned prior to electrode placement. To maximize the access to the median and ulnar nerves from the skin surface, a 2×8 electrode grid was situated collaterally to the vector connecting the medial epicondyle of the humerus and the center of the axilla (Figure 1B). Stable electrode-skin contact was achieved using mild pressure from a custom vice. Participants were reminded to report any discomfort throughout the study. Activation of different electrode pairs resulted in the generation of unique electric fields, which can activate distinct sets of axons producing a variety of muscle activation patterns [11].

A custom MATLAB interface controlled a multi-channel stimulator (STG4008, Multichannel Systems, Reutlingen, Germany) and a switch matrix (Agilent Technologies, Santa Clara, CA). The interface defined the stimulation paradigms of the charge-balanced biphasic square wave stimulus, including its amplitude, frequency, and pulse width. The interface also linked the anode or the cathode of the stimulator to one of sixteen gel-based electrodes using the switch matrix. Although pulse width and frequency were adjustable, these parameters were fixed at 500 µs, respectively [11].

Activation of the finger flexor muscles was recorded using surface EMG. Prior to placement of the EMG electrodes, the forearm and palm were cleaned with alcohol pads to improve the EMG signal quality. An 8×16 channel HD EMG grid (OT Bioelettronica, Torino, Italy) was placed along the anterior portion of the forearm to record the extrinsic flexor muscles [10]. In addition, one 4×8 EMG pad was placed upon the palmar of the hand to record the intrinsic finger muscles. Figure 1A illustrates the general muscle activation pattern in the heat map and the muscle response to a single stimulation pulse. The electrodes located on the EMG pads are 3mm in diameter with an inter-electrode distance of 10 mm. The EMG-USB2+ biosignal amplifier (OT Bioelettronica, Torino, Italy) was used to sample the monopolar EMG signals at a rate of 2048 Hz. The gain and bandwidth of the amplifier were set to 200 and 10-900 Hz, respectively. The common ground and reference electrode were positioned along the wrist and elbow, respectively. The specific location of the electrode pads was specified via palpitation of the forearm and hand muscles as voluntary finger flexion was performed.
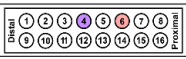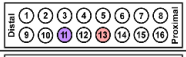
Individual finger forces were recorded using four miniature load cells (SM-200N, Interface, Scottsdale, AZ). Each finger was extended and abducted comfortably to position it atop of each assigned load cell. Velcro straps were wrapped around each finger and load cell to ensure accurate force measurement (Figure 1B). To isolate finger flexion forces, two stiff foam pads were placed on the dorsal and palmar sides of the hand. The forces produced by the index, middle, ring, and pinky were sampled independently at 1000 Hz.

C. Procedures

The experiment began by searching through the stimulation electrode grid for a pair that produced finger flexion without causing discomfort. During grid exploration, the stimulation duration was set to 0.5 seconds of 30 Hz pulses (15 consecutive pulses), in order to pinpoint a pair that prioritized finger flexion over wrist flexion.

Once a viable stimulation pair was identified, a single biphasic pulse was delivered in a stimulation trial (Figure 2A). Prior to the main testing, with increasing stimulation amplitude, we first identified the maximum stimulation amplitude, when the forces became saturated. Five seconds of rest was allocated between stimulation trials to allow time to determine if the force matched the previous value and to prevent potential fatigue. The stimulation amplitude that produced a saturated force level was assigned as the upper bound of the stimulation range, while 0 was selected as the lower bound. The stimulation information for all participants is detailed in Table 1. In this preliminary study, the experiment was performed using two stimulation pairs for subject 1 (Pairs

Figure 2. Diagram illustrating the procedure including the stimulation profile used (A) and representative EMG responses for all channels (B).

Table 1. Stimulation Pair/Range and Fingers Activated

Pair #	Electrode Pair (Cathode / Anode)	Stimulation Range (mA)	Fingers Activated
1	Distal ①②③④⑤⑥⑦⑧ / ⑨⑩⑪⑫⑬⑭⑮⑯ Proximal	0 - 12	All Fingers
2	Distal ①②③④⑤⑥⑦⑧ / ⑨⑩⑪⑫⑬⑭⑮⑯ Proximal	0 - 11	Primarily, Index and Pinky
3	Distal ①②③④⑤⑥⑦⑧ / ⑨⑩⑪⑫⑬⑭⑮⑯ Proximal	0 - 7.5	All Fingers

1 and 2) and one pair for subject 2 (Pair 3).

For each pair in the main experiment, the number of trials was dependent on stimulation range. A step of 0.1 mA was used. Namely a stimulation range of 0-12 mA, such as in Pair 1, would result in 121 stimulation trials with randomized stimulation amplitudes (Figure 2A). A given trial's amplitude was randomly pulled from a pool, ensuring a double-blinded scenario. A 2-second resting time was provided between trials. For each trial, the force produced and EMG were recorded.

D. Data Processing

For each pair, the stimulation levels that resulted in a M-wave and/or H-reflex were identified. Utilizing these levels, EMG across all channels were visualized to determine the time points in which the M-wave and H-reflex primarily began and ended relative to the stimulation timing. These time stamps were used to locate peaks that characterized the M-wave and H-reflex response for a given stimulation level and EMG channel. For each pair, different time stamps were used for the EMG electrode grids on the forearm and the hand.

To quantify the spatial distribution of the muscle activity, heat maps were used to depict the major regions of activation for each pair. The root mean square (RMS) was used to evaluate the overall activation of the hand and forearm muscles when delivering stimulus at 90% of the maximum stimulation amplitude. In addition, heat maps were used to visualize the dispersal of the maximum M-wave and H-reflex responses and M-wave amplitude following the disappearance of the H-reflex. After identifying the channel that generated the maximum H-reflex response, the recruitment curves of the H-reflex and M-wave amplitude (positive peak) were constructed as a function of the stimulation level.

III. RESULTS

We evaluated the 160 channels of EMG generated from all stimulation levels to determine the M-wave and H-reflex responses for a given stimulation pair. Figure 3A & 3E show

the heat map depicting the spatial distribution of the muscle activation at 90% of the max stimulation amplitude when Pairs 1 and 2 were used, respectively. For Pair 1, most of the muscle activity was concentrated along the proximal region of the forearm, while Pair 2 elicited most of the muscle activity along the ulnar region of the forearm. When evaluating the primary location of the maximum M-wave (Figure 3B) and H-reflex (Figure 3C) responses for Pair 1, the location was concentrated along a similar region; however, the H-reflex response had relatively greater activities across more channels along the distal region of the forearm. The activation level in the forearm and hand was similar for the overall EMG and M-wave, but the H-reflex activation was less along the hand than in the forearm. The H-reflex response in a different region suggested that unique muscle compartments may be activated by the afferent pathway. Similar to Pair 1, the spatial distribution of the muscle activity produced by Pair 2 was similar for the M-wave (Figure 3F) and overall EMG. Contrarily, the H-reflex response (Figure 3G) from Pair 2 was not concentrated along a specific region. In addition, the level of H-reflex activation was substantially lower, compared to Pair 1. Lastly. Figure 3D shows the recruitment curve of the M-wave and H-reflex amplitude at various stimulation levels when stimulating Pair 1. The M-wave increased along a sigmoidal shape from approximately 7 mA stimulation amplitude to 12 mA. In contrast, the H-reflex increased from approximately 6 mA stimulation, peaked around 7.5 mA, and then decreased to 0 at around 8 mA. In addition, the maximum H-reflex amplitude only reached to approximately 5% of the maximum M-wave amplitude.

Figure 4 shows the muscle activation when stimulation Pair 3 was used. The overall muscle activation pattern (Figure 4A) and M-wave response (Figure 4B) arose at similar regions along the forearm and hand. In contrast, the M-wave distribution (Figure 4D) just after the absence of H-reflex was different from the maximum M-wave. In addition, the H-reflex distribution was observed in a rather distinct location (Figure 4C). Figure 4E shows the recruitment curve of the M-wave and H-reflex. The shape of the two curves was similar across Pairs 1 and 3. However, the H reflex response reached a peak value of approximately 20% of the maximum
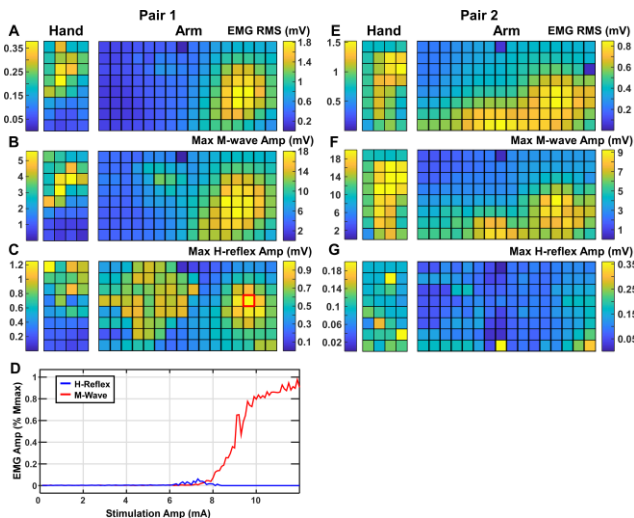

Figure 3. Heat maps illustrating the EMG response with stimulation Pairs 1 and 2. For each Pair, the EMG RMS at 90% of the stimulation maximum (A & E), maximum M-wave (B & F), and maximum H-reflex (C & G) for each channel are depicted. Panel D illustrates the M-wave and H-reflex recruitment curve as a function of the stimulation amplitude via Pair 1. For Pair 2, the H-reflex response was minimum compared to that reported in Pair 1, resulting in substantially lower amplitudes across the arm pads.
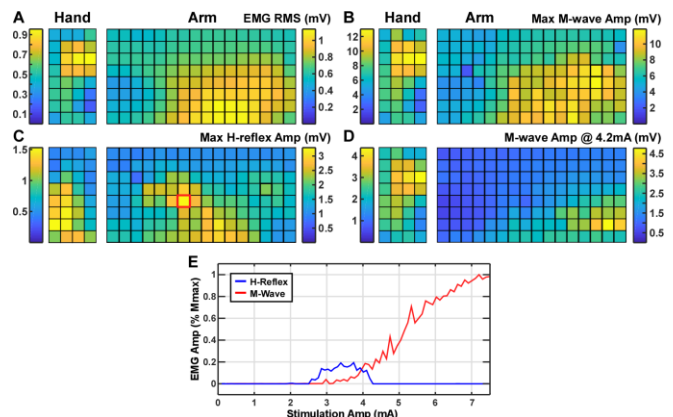

Figure 4. Heat maps illustrating the EMG response with stimulation Pair 3. The EMG RMS at 90% of the stimulation maximum (A), maximum M-wave (B), maximum H-reflex (C), and M-wave following the disappearance of the H reflex (D) for each channel are depicted. The H-reflex amplitude is evident in this case. E: The M-wave and H-reflex recruitment curve as a function of the stimulation amplitude.

M-wave, which was substantially larger than in Pair 1.

IV. Discussion

This preliminary study sought to evaluate the distribution of M-wave and H-reflex in intrinsic and extrinsic finger muscles with various stimulation location and intensity using TNS. HD EMG along the hand and forearm was obtained to depict the H-reflex evoked via secondary activation of the Ia afferent pathway and the M-wave elicited directly from the efferent fibers. Our results showed that stimulation location and intensity affected Ia fiber recruitment causing varied responses across conditions. The diverse H-reflex responses across stimulation parameters (location and intensity) suggest that alteration of these factors can improve the extent of Ia afferent fiber recruitment during evoked muscle activation. Greater afferent recruitment can lead to more physiological activation of targeted muscles, potentially leading to sustained muscle activation over time.

Our results showed that H-reflex response can be altered based on the stimulation location and intensity. By utilizing HD EMG, we were able to pinpoint the localized region of activation for the M-wave and H-reflex across the intrinsic and extrinsic finger muscles. The primary activation region across the M-wave (maximum and following H-reflex disappearance) and overall EMG RMS were similar; however, discrepancies were present when comparing these regions to the H-reflex. This implies that Ia fibers are likely activating motoneurons innervating unique muscle regions. Across all pairs, Ia fiber recruitment varied with the greatest activity in Pair 3. Although the individual characteristics of the participants may have been a factor when comparing Pair 1 to Pair 3, the effects of altering the stimulation location are clearly seen across Pairs 1 and 2. In addition, the shapes of the M-wave and H-reflex curves were consistent across participants. Nonetheless, future work is vital to expand our understanding of the H-reflex response across subjects and muscle groups.

1-Hz pulses were used to visualize the motor response at various stimulation intensities; however, to evoke sustained motor output, higher frequency pulses would be employed to elicit continued activation of the H-reflex. Prior work suggests that post-activation depression of the H reflex occurs in upper limb muscles [16]. Contrarily, recent work has shown that TNS elicits sustained H-reflex activity without obvious signs of decay [17]. The increase in H-reflex is believed to be due to the increased excitability of the spinal reflex caused by the repetitive stimulation, suggesting higher H-reflex amplitudes than those observed in this study may be achievable through continued stimulation.

Several limitations of this current study include a lack of post-stroke participants, a small sample size, and a small number of examined stimulation pairs per subject. First, previous work has shown that TNS can produce similar hand motions in neurologically intact and stroke participants [12]. In addition, prior work has shown that muscular activation (M-wave and H-reflex amplitude) responded to increasing stimulus in a similar manner in neurologically intact and post-stroke participants [13]. Our stimulation and recording techniques can be used to further quantify the excitability of efferent and afferent pathways of impaired limbs. In regard to the sample size and the number of pairs per subject, this study was conducted to provide a preliminary evaluation of the response to increasing stimulus and varied stimulation locations. Future work will expand this evaluation to include a larger population and greater number of stimulation locations.

In conclusion, this preliminary study provides evidence that varied stimulation intensity and location can regulate the H-reflex recruitment. Using this information, stimulation parameters can be exploited to maximize the involvement of afferent pathways with TNS, potentially promoting greater rehabilitative outcomes of individuals with neuromuscular conditions.

References

[1] R. Bohannon, "Muscle strength and muscle training after stroke," *J. Rehabil. Med.*, vol. 39, no. 1, pp. 14–20, 2007.

[2] E. J. Benjamin *et al.*, *Heart disease and stroke statistics - 2018 update: A report from the American Heart Association*, vol. 137, no. 12. 2018.

[3] D. T. Wade *et al.*, "The hemiplegic arm after stroke: measurement and recovery.," *J. Neurol. Neurosurg. Psychiatry*, vol. 46, no. 6, pp. 521–524, Jun. 1983.

[4] A. Sunderland *et al.*, "Arm function after stroke. An evaluation of grip strength as a measure of recovery and a prognostic indicator.," *J. Neurol. Neurosurg. Psychiatry*, vol. 52, no. 11, pp. 1267–1272, Nov. 1989.

[5] F. Quandt and F. C. Hummel, "The influence of functional electrical stimulation on hand motor recovery in stroke patients: a review," *Exp. Transl. Stroke Med.*, vol. 6, no. 1, Dec. 2014. Art. no. 9.

[6] C. S. Bickel *et al.*, "Motor unit recruitment during neuromuscular electrical stimulation: a critical appraisal," *Eur. J. Appl. Physiol.*, vol. 111, no. 10, pp. 2399–2407, Oct. 2011.

[7] A. J. Bergquist *et al.*, "Neuromuscular electrical stimulation: implications of the electrically evoked sensory volley," *Eur. J. Appl. Physiol.*, vol. 111, no. 10, pp. 2409–2426, Oct. 2011.

[8] A. J. Bergquist *et al.*, "Motor unit recruitment when neuromuscular electrical stimulation is applied over a nerve trunk compared with a muscle belly: triceps surae," *J. Appl. Physiol.*, vol. 110, no. 3, pp. 627–637, Mar. 2011.

[9] H. Shin *et al.*, "Delayed fatigue in finger flexion forces through transcutaneous nerve stimulation," *J. Neural Eng.*, vol. 15, no. 6, Dec. 2018, Art. no. 066005.

[10] Y. Zheng *et al.*, "Automatic detection of contracting muscle regions via the deformation field of transverse ultrasound images: a feasibility study," *Ann. Biomed. Eng.*, vol. 49, pp. 354–366, Jan. 2021.

[11] H. Shin and X. Hu, "Multichannel Nerve Stimulation for Diverse Activation of Finger Flexors," *IEEE Trans. Neural Syst. Rehabil. Eng.*, vol. 27, no. 12, pp. 2361–2368, Dec. 2019.

[12] H. Shin *et al.*, "Variation of Finger Activation Patterns Post-stroke Through Non-invasive Nerve Stimulation," *Front. Neurol.*, vol. 9, Dec. 2018, Art. no. 1101.

[13] C. P. Phadke *et al.*, "Upper-extremity H-reflex measurement post-stroke: Reliability and inter-limb differences," *Clin. Neurophysiol.*, vol. 123, no. 8, pp. 1606–1615, Aug. 2012.

[14] D. Burke, "Clinical uses of H reflexes of upper and lower limb muscles," *Clin. Neurophysiol. Pract.*, vol. 1, pp. 9–17, 2016.

[15] A. M. Stowe *et al.*, "Between-day reliability of upper extremity H-reflexes," *J. Neurosci. Methods*, vol. 170, no. 2, pp. 317–323, May 2008.

[16] C. Rossi-Durand *et al.*, "Comparison of the depression of H-reflexes following previous activation in upper and lower limb muscles in human subjects," *Exp. Brain Res.*, vol. 126, no. 1, pp. 117–127, 1999.

[17] Y. Zheng and X. Hu, "Elicited Finger and Wrist Extension Through Transcutaneous Radial Nerve Stimulation," *IEEE Trans. Neural Syst. Rehabil. Eng.*, vol. 27, no. 9, pp. 1875–1882, Sep. 2019.